tion. A drop of Nylon 6,6–isopropanol suspension was deposited on a carbon-coated TEM grid. The grid was shadowed with a thin layer of platinum. A JEOL (1200 EX II) TEM with an accelerating voltage of 120 kV was used and calibration of the SAED spacing was done using TlCl standards. A Digital Instrument Nanoscope IIIA was used for AFM experiments. A drop of Nylon 6,6 crystal suspension was deposited on a carbon-coated glass slide. The force used by the cantilever was light enough to limit damage to the sample, yet obtain accurate surface features. The scanning rate was 1–3 Hz for the low magnification images (512 × 512 pixels per image).

Received: July 2, 2003
Final version: December 18, 2003

[1] S. Ijimi, *Nature* **1991**, *354*, 53.
[2] R. Tenne, *Prog. Inorg. Chem.* **2001**, *50*, 269.
[3] P. M. Ajayan, O. Stephan, P. Redlich, C. Colliex, *Nature* **1995**, *375*, 564.
[4] J. Goldberger, R. He, Y. Zhang, S. Lee, H. Yan, H.-J. Choi, P. Yang, *Nature* **2003**, *422*, 599.
[5] M. Steinhart, J. H. Wendorff, A. Greiner, R. B. Wehrspohn, K. Nielsch, J. Schilling, J. Choi, U. Gosele, *Science* **2002**, *296*, 1997.
[6] M. Bognitzki, H. Hou, M. Ishaque, T. Frese, M. Hellwig, C. Schwarte, A. Schaper, J. H. Wendorff, A. Greiner, *Adv. Mater.* **2000**, *12*, 637.
[7] H. Hou, Z. Jun, A. Reuning, A. Schaper, J. H. Wendorff, A. Creiner, *Macromolecules* **2002**, *35*, 2429.
[8] A. Keller, *Rep. Prog. Phys.* **1968**, *31*, 623.
[9] F. Khoury, E. Passaglia, *Treatise Solid State Chem.* **1976**, *3*, 335.
[10] P. H. Geil, *Polymer Single Crystals*, Krieger Publishing, Huntingdon, NY **1973**.
[11] D. C. Bassett, F. C. Frank, A. Keller, *Philos. Mag.* **1963**, *8*, 1739.
[12] B. Lotz, A. Gonthier-Vassal, A. Brack, J. Magoshi, *J. Mol. Biol.* **1982**, *156*, 345.
[13] C. Y. Li, S. Z. D. Cheng, J. J. Ge, F. Bai, J. Z. Zhang, I. K. Mann, L. C. Chien, F. W. Harris, B. Lotz, *J. Am. Chem. Soc.* **2000**, *122*, 72.
[14] C. Y. Li, S. Z. D. Cheng, J. J. Ge, F. Bai, J. Z. Zhang, I. K. Mann, F. W. Harris, L. C. Chien, D. Yan, T. He, B. Lotz, *Phys. Rev. Lett.* **1999**, *83*, 4558.
[15] V. F. Holland, R. L. Miller, *J. Appl. Phys.* **1964**, *35*, 3241.
[16] A. S. Vaughan, *J. Mater. Sci.* **1993**, *28*, 1805.
[17] B. Lotz, A. Thierry, S. Schneider, *C. R. Acad. Sci., Ser. IIc: Chim.* **1998**, *1*, 609.
[18] Personal communication: Prof. Geil has shown us his early TEM images of Nylon 6,6, single crystals, some of which are also scrolled.
[19] P. H. Geil, *J. Polym. Sci.* **1960**, *44*, 449.
[20] C. W. Bunn, E. V. Garner, *Proc. R. Soc. London A* **1947**, *189*, 39.
[21] V. F. Holland, *Makromol. Chem.* **1964**, *71*, 204.
[22] H. M. White, I. L. Hosier, D. C. Bassett, *Macromolecules* **2002**, *35*, 6763.
[23] P. Dreyfuss, A. J. Keller, *J. Macromol. Sci,. Phys.* **1970**, *B4*, 811.
[24] J. L. Koenig, M. C. Agboatwalla, *J. Macromol. Sci., Phys.* **1968**, *B2*, 391.

Electrospray-Assisted Fabrication of Uniform Photonic Balls**

By *Jun Hyuk Moon*, *Gi-Ra Yi*, *Seung-Man Yang*,* *David J. Pine*, and *Seung Bin Park*

Arrays of close-packed, equal-sized microspheres have been used as templates for the micro- and nano-fabrication of optical materials. Colloidal suspensions of such monodisperse spheres can be especially useful in making optical materials because they can self-organize into ordered, hexagonally packed crystalline lattices in two or three dimensions.[1] These opaline lattices can exhibit optical insulating behavior (i.e., they can have a photonic bandgap (PBG)), similar to semiconductors in electronic devices, and are called photonic crystals. The optical insulating behavior of photonic crystals arises from the cooperative scattering of light from the ordered array of particles.[2] However, these opaline structures do not have a full PBG but only a few narrow stop bands. It is known that inverse opaline structures exhibit wider stop bandgaps, and can possess a full PBG when the refractive index contrast exceeds about 2.8. The inverse opaline structures are formed by infiltrating dielectric material into the interstices between the colloidal spheres and then dissolving the spheres away.[3] This produces an ordered foam of spherical cavities. The stop bands of opals or inverse opals with a face-centered cubic arrangement can be exploited to modify the spontaneous emission of organic dyes and semiconductor nanocrystals embedded in the voids of the colloidal crystals.[4]

One of the important issues in the design of photonic crystals is the control of their uniformity in size and shape. This is required for the development of photonic devices, including waveguides and optical components, such as microlenses and beam splitters.[5–7] For other applications, photonic crystals in the form of colloidal clusters could be especially valuable, for example, as light scatterers, light diffusers, and pigments for electronic paper and electronic displays.[8–10] The practical use of these materials, however, requires the production of large quantities of *monodisperse* colloidal clusters.

Here, we report a simple, *single-step* synthetic route for the generation of uniform colloidal aggregates and their inverse structures by electrospraying an aqueous colloidal suspension. Hereafter, both our opaline balls and their inverse structures

[*] Prof. S.-M. Yang, J. H. Moon, Dr. G.-R. Yi, Prof. S. B. Park
Department of Chemical and Biomolecular Engineering
Korea Advanced Institute of Science and Technology
373-1 Guseong-dong, Yuseong-gu, Daejeon 305-701 (South Korea)
E-mail: smyang@kaist.ac.kr
Prof. D. J. Pine
Department of Chemical Engineering and Materials Department
University of California, Santa Barbara
Santa Barbara, CA 93106-5080 (USA)

[**] This work was supported by the "National R&D Project for Nano Science and Technology" of the Ministry of Science and Technology. Partial support from the Brain Korea 21 Program and CUPS-ERC are also acknowledged.

 DOI: 10.1002/adma.200305446

ADVANCED MATERIALS

will be called "photonic balls". In previous work, several approaches have been successfully used to produce photonic balls, including microfluidic chips,[11] micropipette injection,[12] and double templating.[13] Although these approaches produce monodisperse photonic balls, they are all microscale processes and have some limitations for practical applications. In addition, the microfluidic chips and the micropipette injection produce photonic balls from aqueous suspension droplets in an oil phase, which then has to be removed for subsequent processing. Therefore, it remains a challenge to mass-produce uniform photonic balls in a cost-efficient and controllable way. Our approach, based on electrospraying, is the first report of the large-scale production of uniform photonic balls. The basic idea is to fabricate well-organized photonic balls of colloidal spheres from aqueous suspension droplets that contain either the polymer latex beads for photonic balls or the mixture of the polymer latex beads and nanometer-sized ceramic particles for inverse photonic balls (see Scheme 1). Among the most important advantages of our electrospray technique are that aqueous emulsion drops are produced in air and that the compressible capillary force is relatively large compared to that in water-in-oil emulsions. Because the capillary force is responsible not only for the spherical shape of photonic balls but also for close packing of the spherical polymeric latex beads, the shape, size, and internal arrangement of photonic balls are controllable over a wide range and within a very narrow distribution.[14] Furthermore, the droplets produced have a net surface charge that prevents droplets from coalescing.

Typically the different modes of generating droplets by electrospraying a homogeneous liquid are classified into three distinct regimes: 1) dripping, 2) emission of droplets from the liquid cone, and 3) jet-breakup modes, depending on the electric-field strength and liquid flow-rate.[15] Under the action of a direct current (DC) electric field, however, it is difficult to generate uniform-sized droplets of a highly conducting liquid in a controllable manner through the typical droplet breakup modes. This is because of the short charge-relaxation time of a conducting liquid, which induces an electrostatic force in a DC field. Under these conditions, the electric force either builds up to such an extent that the liquid breaks up before a drop can completely form and break away, or the axis of a droplet that is forming will shift from side to side due to an instability caused by lateral electric forces.[16] By contrast, an alternating current (AC) electric field reduces the formation of the surface charge that drives the first instability and also suppresses the onset of the second (lateral) instability.[17] By virtue of the highly conducting properties of the aqueous suspensions that were used in the present study, an AC electric field was employed to generate uniform-sized droplets. Usually, the method using a DC field produces droplets with a relatively wide size distribution by forming liquid jets that subsequently break up into droplets through the Rayleigh instability.[18] Here, we present an alternative field-enhanced dripping method that is simpler and provides more control over the droplet size by changing the strength and frequency of the electric field.

As shown in Scheme 1A, a nitrogen pressure head was used to force the suspension through a 160 μm diameter metal needle. The pressure of nitrogen was adjusted to control the flow rate over a range from 0.15 to 0.35 mL min^{-1}. The needle was connected to an alternating electric potential of several kilovolts relative to a ground electrode plate. When the electric field was applied, the electrohydrodynamic force elongated and sharpened the liquid meniscus formed at the outlet of the nozzle and detached a droplet from the meniscus. Under an AC field, the formation of the droplet was synchronized with the electric field. The formation of droplets from a homogeneous liquid phase is governed primarily by the frequency and strength of the electric field, the liquid flow-rate, and the surface tension. In the present case, however, the liquid phase was an aqueous suspension of polystyrene (PS) beads of a few hundred nanometers diameter. Therefore, the drop formation was also influenced by the particle loading. To facilitate the generation of uniform-sized suspension droplets, the PS bead loading was kept below 10 vol.-%.

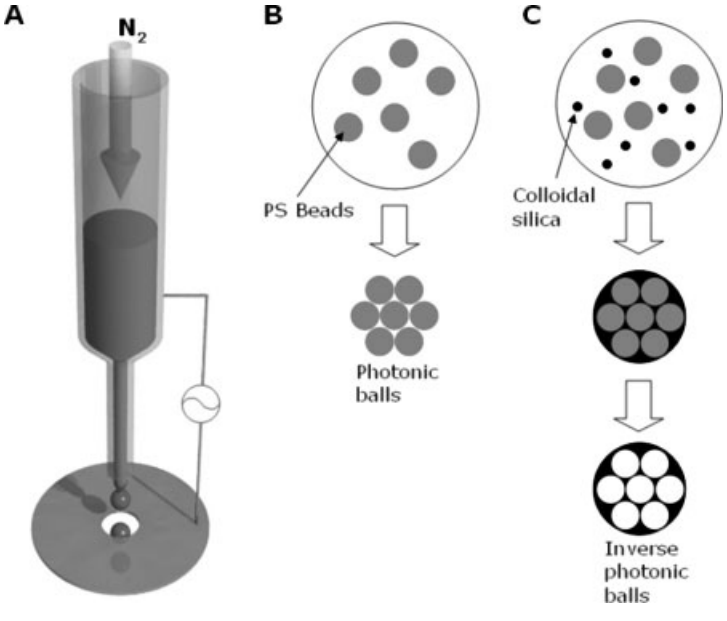

Scheme 1. A) Schematic of electrospray for suspension droplet generation. B) Scheme for the preparation of opaline photonic balls. C) Scheme for the preparation of inverse photonic balls.

The field strength and surface tension can be parameterized to a dimensionless electric Bond number $B_e = (\varepsilon V^2/d\sigma)$, which is the ratio of deforming stress from the electric field to restoring force provided by the interfacial tension. Here, ε is the permittivity of air, V is the electric-field strength, d is the diameter of a droplet attached to the needle, and σ is the surface tension. Notz and Basaran have shown that the volume of a droplet detached from the needle decreases linearly with increasing Bond number.[19] As the deforming electric stress increases, so does the contribution from the interfacial tension. Thus, the size of a detached droplet decreases. It should be noted that the

field-induced stress was synchronized with the oscillating electric field, but at double the frequency. However, the synchronization with the field, which was required for the generation of monodisperse droplets, occurred only below a certain electric-field frequency, which for our experiments was in the range of 30–200 Hz, depending on the field strength. Similarly, the electric-field strength also could not be increased above a certain level, typically about 7.0 kV cm^{-1}, since an excessively high electric field led to the formation of satellite droplets and multi-jets, thereby greatly increasing the polydispersity of the size of the droplets.

First, we consider the preparation of opaline photonic balls from an aqueous suspension of PS beads shown in Scheme 1B. In Figure 1a, the diameter of the suspension droplets is plotted against the square of the electric-field strength for various flow rates and field frequencies. The square of the electric-field strength is proportional to the electric Bond number. As expected, the droplet size decreased linearly as the electric Bond number was increased for a given liquid flow-rate. Figure 1b shows the diameter of the suspension drop as a function of the electric-field frequency for two different field strengths. It can be seen that the effect of changing the frequency on the drop size diminished as the electric field became stronger. This is because the meniscus-sharpening saturated when the electric-field strength was increased to the limiting value for the generation of uniform-sized droplets.

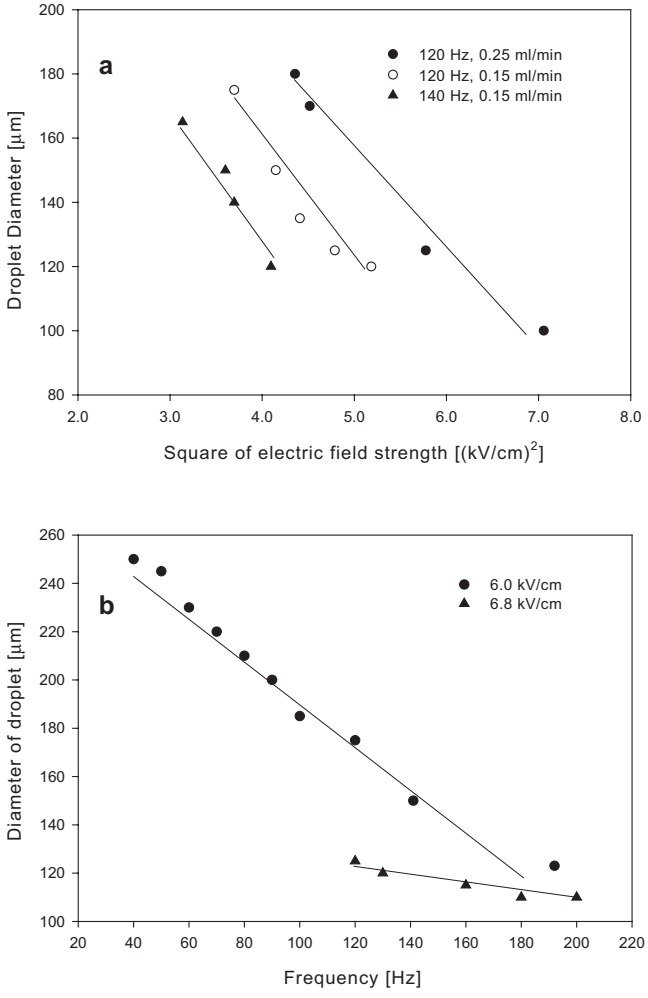

Figure 1. a) Diameter of uniform-sized suspension droplets formed by electrospray as a function of the electric-field strength for various frequencies and flow rates. b) Diameter of uniform-sized suspension droplets formed by electrospray as a function of the electric-field frequency.

The suspension droplets were issued from the needle through air at the rate of 60–400 Hz. Here, the PS loading was kept between 5 and 10 vol.-% to ensure monodisperse photonic balls with diameters ranging from 60 to 100 μm. The PS beads inside the suspension droplets self-organized into photonic balls spontaneously when the aqueous solvent was removed from the droplets by evaporation. In this system, capillary forces provide a compressive force that is spherically symmetrical and ultimately leads to an arrangement of the particles. The capillary force thus close-packs the PS beads into their final configuration, and van der Waals' forces subsequently cement the PS beads together. In addition, coalescence between droplets did not occur due to the surface charge of the droplets. Therefore, the size of the photonic balls could be controlled by the particle loading as well as the diameter of the suspension droplets. As shown in the scanning electron microscopy (SEM) image in Figure 2a, the photonic balls consist of closely packed PS beads in a face-centered cubic arrangement due to a relatively large capillary force at the air–water interface.

To examine the optical properties, the opaline photonic balls were dispersed in silicone oil. The optical reflectivity spectrum of the photonic balls depends on the size of the PS beads. The photonic balls exhibit blue, green, and red reflection colors as the PS bead diameter increases from 180 nm to 260 nm (see Figs. 2b–d). The transmission spectra of visible light through the photonic balls dispersed in the silicone oil are reproduced in Figure 3a. The reflections appear around 430, 530, and 650 nm for three different sizes (180, 230, and 260 nm) of

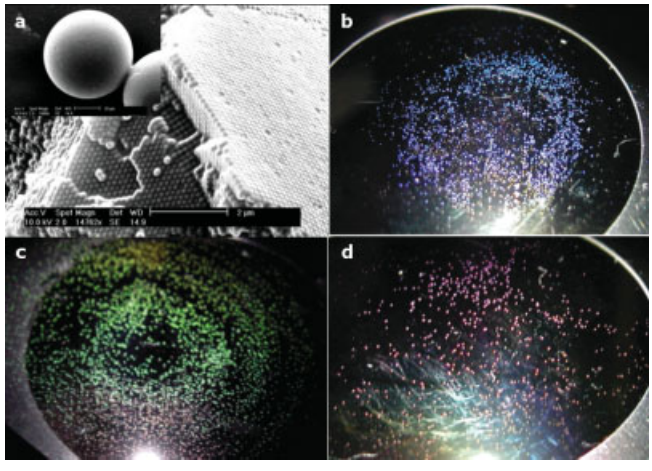

Figure 2. a) High-magnification SEM image of the cross section and surface of opaline photonic balls. The inset shows an SEM image of the opaline photonic balls. b–d) The opaline photonic balls exhibit the reflection color of blue, green, and red with constituent PS beads of 180, 230, and 260 nm in diameter, respectively.

ADVANCED MATERIALS

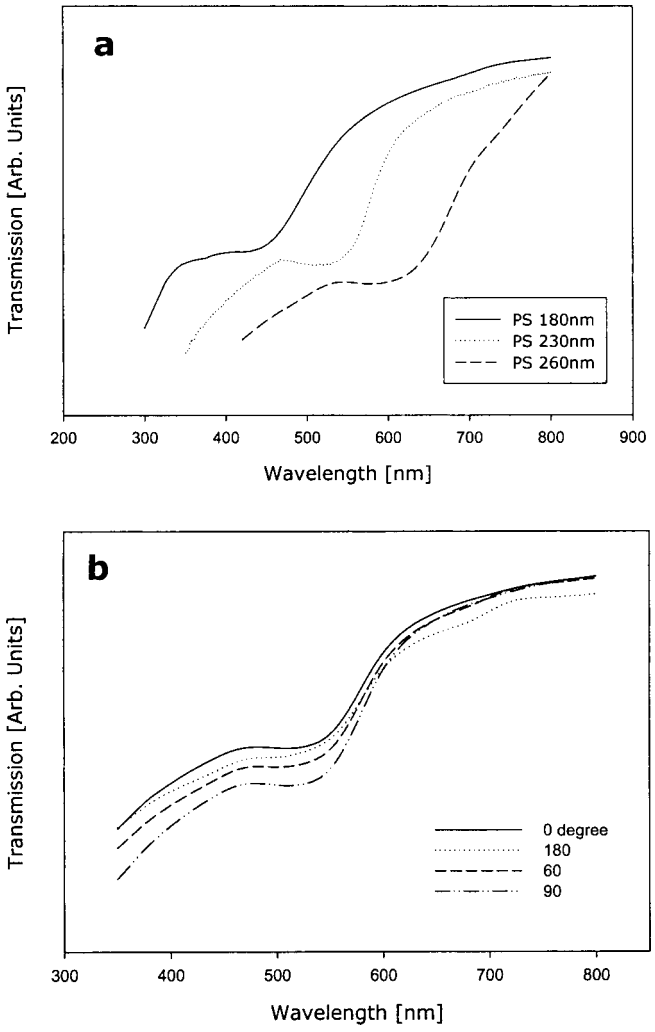

Figure 3. a) Transmission spectra of opaline photonic balls that consist of the PS beads of three different sizes. b) Transmission spectra at different incident angles of opaline photonic balls that consist of PS beads of 230 nm.

building-block PS beads, respectively. Because the spherical surface of the photonic ball is the (111) plane of the fcc lattice, the angle between the incident beam and the surface is not the same over the surface of the ball, resulting in a rather broad reflection band.[20] However, the major reflection occurs for the light coming through the (111) direction, in which the photonic ball has a stop band. The stop bands (or the reflection peak locations) are consistent with the estimates from Bragg's law for the refractive indices (1.60 for PS and 1.40 for silicone oil) and the diameters of the PS beads.[21,22] Figure 3b shows the transmission spectrum at different incident angles of photonic balls containing 230 nm PS beads. As expected, the reflection peak is independent of the incident angles due to the spherical symmetry of the internal and external structures of the photonic balls. Therefore, although a spherical surface of the photonic ball broadens the reflection peak due to the variation of the incident angle relative to the (111) plane over the surface, the sphericity produces an identical optical reflectivity spectrum in all directions, which is in contrast to the case of a plane colloidal photonic crystal film.[23]

Now we consider the preparation of inverse opaline photonic balls (Scheme 1C), in which the aqueous suspension contained PS beads of 260 nm and nano-sized silica particles. The PS particles self-assembled in the same manner as described previously. The nano-sized silica particles were able to infiltrate into the interstitial sites between the large PS beads during the evaporation of water. After a burn-out process, as used in a conventional templating process, uniform inverse structures of photonic balls were successfully produced, as shown in Figure 4a. The pore size was reduced to 240 nm due to the shrinkage (about 8 %) during heat treatment. Meanwhile, as seen from Figure 4b, the pores are interconnected and extended to the inside of the inverse opaline photonic

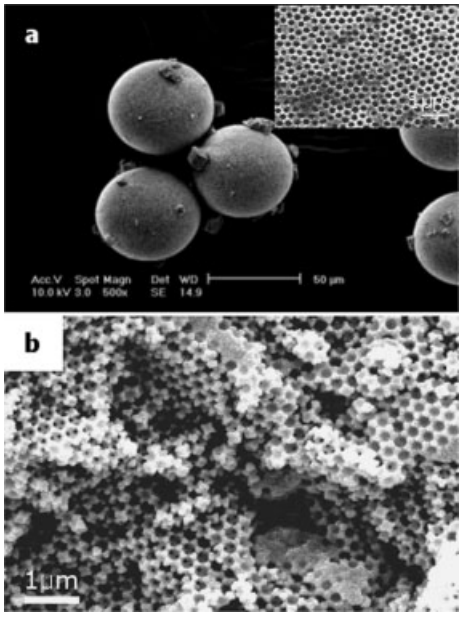

Figure 4. a) SEM image of inverse opaline photonic balls. The matrix medium of these structures consists of the consolidated silica nanoparticles. The inset shows a high-magnification image of the surface of the inverse opaline photonic balls. b) A high-magnification SEM image shows the ordered pore structures inside.

ball, indicating the ordering of the PS beads. The transmission spectrum of the inverse photonic balls is shown in Figure 5a. The optical reflection appears at around 450 nm, consistent with Bragg's law for the refractive indices (1.47 for silica and 1.00 for air), and is matched with the reflected color observed through an optical microscope (Fig. 5b).

In summary, we have demonstrated a simple promising approach to produce uniform photonic balls in a cost-efficient and controllable way under an AC electric field. The size of the suspension droplets was easily controlled by the strength and frequency of the AC electric field, which, in turn, adjusted the size of the prepared photonic balls. The size of the prepared balls can also be controlled using the particle loading of the suspension. Moreover, inverse opaline photonic balls were

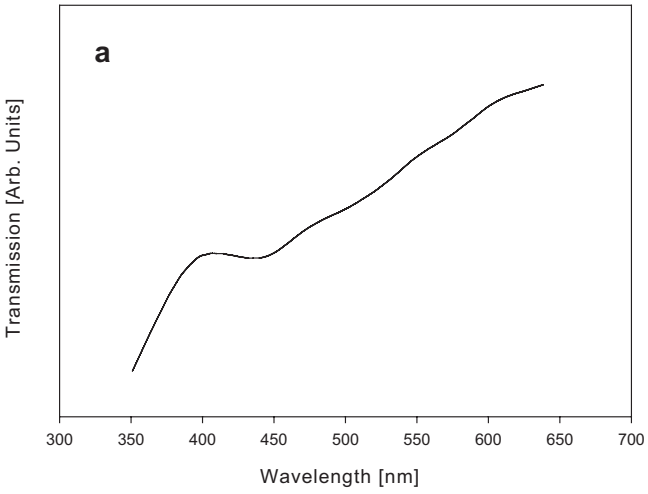

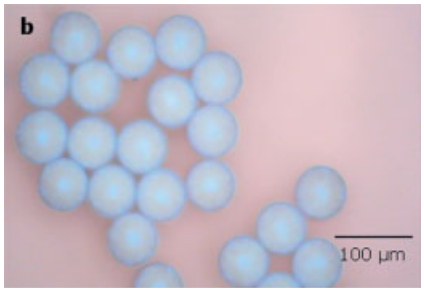

Figure 5. a) Transmission spectra of inverse opaline photonic balls with ordered spherical pores of 240 nm in diameter. b) An optical microscope image of inverse opaline photonic balls showing the violet–blue color.

produced by adding nano-sized silica particles to the PS bead suspension and then performing a standard templating process. Among the most important features of our photonic balls is that they display an angle-independent specific color, which depends only on the size of the PS beads, or their replica pores, and the refractive index contrast. Therefore, our photonic balls are very promising as color pigments for reflection-based displays. In addition, the present method can be extended to the mass production of non-isotropic colloidal building blocks to create new types of photonic crystals.[14]

Experimental

Preparation of the Colloidal Suspension: Monodisperse polystyrene (PS) latex particles with diameters ranging from 180 to 260 nm were synthesized by emulsifier-free emulsion polymerization. Nano-sized silica particles were purchased from Aldrich (Ludox HS-40). HS-40 has a mean particle size of 30 nm at 40 wt.-%. For the binary colloidal system, 10 vol.-% PS particles and 10 vol.-% silica particles were mixed with an equal volume fraction.

Fabrication of Photonic Balls by Electrospray: The suspension was injected into a syringe fitted with a metal needle (Hamilton, Metal hub needle with blunt end, 160 µm in diameter). The flow out of the syringe was controlled by varying the nitrogen pressure. The electric-field strength for the stable generation of suspension droplets was in a range from 3 to 7 kV; the frequency was kept below 200 Hz for the required synchronization with the rate of formation of the suspension droplets. The suspension droplets were produced at a rate double the AC field frequency. The drop size was uniform and the polydispersity was within 1 %, as estimated from an image analysis. During the evaporation of solvent water from the suspension droplets, the PS beads self-organized into close-packed, spherical photonic balls. For the inverse opaline photonic balls, a binary colloidal suspension of larger PS beads and nano-sized silica was sprayed into air. The silica-infiltrated photonic balls were heated slowly to 500 °C for 8 h to remove the templating PS beads, leaving behind the ordered pores.

Characterization: Images of the prepared opaline and inverse opaline photonic balls were obtained by SEM (Philips, XL30) at 10 kV. The samples for SEM were coated with Au to render them conductive. For measuring the optical properties, a large number (10^5–10^6) of the photonic balls were dispersed in silicone oil in a 5 mL glass tube, and UV-vis spectroscopy (Cary 500) in the range of visible light was used. Transmission spectra at different angles were obtained using a rotating sample mount.

Received: May 26, 2003
Final version: November 11, 2003

[1] Y. Xia, B. Gates, Z.-Y. Li, *Adv. Mater.* **2001**, *13*, 409.
[2] S. G. Johnson, J. D. Joannopoulos, *Photonic Crystals: The Road from Theory to Practice*, Kluwer Academic Publishers, Norwell, MA **2002**, pp. 11–22.
[3] J. E. G. J. Wijnhoven, W. L. Vos, *Science* **1997**, *281*, 802.
[4] D. Wang, A. L .Rogach, F. Caruso, *Chem. Mater.* **2003**, *15*, 2724.
[5] E. Chow, S. Y. Lin, S. G. Johnson, P. R. Villeneuve, J. D. Joannopoulos, J. R. Wendt, G. A. Vawter, W. Zubrzycki, H. Hou, A. Alleman, *Nature* **2000**, *407*, 983.
[6] M. Bayindir, B. Temelkuran, E. Ozbay, *Appl. Phys. Lett.* **2000**, *77*, 3902.
[7] P. Halevi, A. A. Krokhin, J. Arriaga, *Appl. Phys. Lett.* **1999**, *75*, 2725.
[8] a) O. D. Velev, A. M. Lenhoff, E. W. Kelar, *Science* **2000**, *287*, 2240. b) G.-R. Yi, J. H. Moon, S.-M. Yang, *Adv. Mater.* **2001**, *13*, 1185.
[9] a) Y. Lu, H. Fan, A Stump, T. Ward, T. Rieker, C. J. Brinker, *Nature* **1999**, *398*, 223. b) F. Iskandar, Mikrajuddin, K. Okuyama, *Nano Lett.* **2001**, *1*, 231.
[10] B. Comiskey, J. D. Albert, H. Yoshizawa, J. Jacobson, *Nature* **1998**, *394*, 253.
[11] G.-R. Yi, V. N. Manoharan, S. Klein, K. R. Brzezinska, D. J. Pine, F. F. Lange, S.-M. Yang, *Adv. Mater.* **2002**, *14*, 1137.
[12] G.-R. Yi, J. H. Moon, V. N. Manoharan, D. J. Pine, S.-M. Yang, *J. Am. Chem. Soc.* **2002**, *124*, 13 354.
[13] G.-R. Yi, T. Thorsen, V. N. Manoharan, M.-J. Hwang, D. J. Pine, S. R. Quake, S.-M. Yang, *Adv. Mater.* **2003**, *15*, 1300.
[14] V. N. Manoharan, M. T. Elsesser, D. J. Pine, *Science* **2003**, *301*, 483.
[15] W. Balachandran, W. Machowski, C. N. Ahmad, *IEEE Trans. Ind. Appl.* **1994**, *30*, 850.
[16] a) A. Jaworek, A. Krupa, *J. Aerosol Sci.* **1999**, *30*, 837. b) I. Hayati, A. I. Bailey, T. F. Tadros, *Nature* **1986**, *319*, 41.
[17] a) W. Balachandran, W. Machowski, C. N. Ahmad, *IEEE Trans. Ind. Appl.* **1994**, *30*, 850. b) Z. A. Huneiti, W. Balachandran, W. W. Machowski, *IEEE Trans. Ind. Appl.* **1998**, *34*, 279.
[18] a) M. Sato, *J. Electrostatics* **1984**, *15*, 237. b) K. Tang, A. Gomez, *J. Aerosol Sci.* **1994**, *25*, 1237. c) D.-R. Chen, D. Y. H. Pui, S. L. Kaufman, *J. Aerosol Sci.* **1995**, *26*, 963.
[19] P. K. Notz, O. A. Basaran, *J. Colloid Interface Sci.* **1995**, *161*, 389.
[20] a) R. C. Schroden, M. Al-Daous, C. F. Blanford, A. Stein, *Chem. Mater.* **2002**, *14*, 3305. b) C. F. Blanford, R. C. Schroden, M. Al-Daous, A. Stein, *Adv. Mater.* **2001**, *13*, 26.
[21] M. Born, E. Wolf, *Principles of Optics*, 7th ed., Cambridge University Press, Cambridge **1999**.
[22] S. H. Park, Y. Xia, *Langmuir* **1999**, *15*, 266.
[23] M. Allard, E. H. Sargent, E. Kumacheva, O. Kalinina, *Opt. Quantum Electron.* **2002**, *34*, 27.

